Electronic Supporting Information

Anchoring copper nanoclusters to Zn-containing hydroxy double salt: construction of 2D surface confinement induced enhanced emission toward bio-enzyme sensing and light-emitting diode fabrication

Jinlan Yang [a], Zheng Li [a] and Qiong Jia *[ab]

[a] *College of Chemistry, Jilin University, Changchun 130012, China*

[b] *Key Laboratory for Molecular Enzymology and Engineering of Ministry of Education, School of Life Sciences, Jilin University, Changchun 130012, China*

Corresponding author: Professor Qiong JIA

Email address: jiaqiong@jlu.edu.cn

CONTENTS

Experimental Section

Chemical and materials

ZnO, $Zn(NO_3)_2 \cdot 6H_2O$, $Cu(NO_3)_2$, $Mg(NO_3)_2 \cdot 6H_2O$, $Al(NO_3)_3 \cdot 9H_2O$, HNO_3, urea, $NaNO_3$, NaOH, KCl, NaCl, $MgCl_2$, $CaCl_2$, and Na_3PO_4 were purchased from Beijing Chemical Works (Beijing, China). Cysteine (Cys), glutathione (GSH), *β*-glucuronidase (GLU, ≥ 10^8 $U \cdot L^{-1}$), 4-nitrophenyl-*β*-D-glucuronide (PNPG), hyaluronidase (HAase), acetylcholinesterase (AChE), casein (CS), thrombin (Thr), glutathione reductase (GR), lysozyme (Lys), and trypsin (Try) were obtained from Sigma-Aldrich Company (St. Louis, MO, USA). Polydimethylsiloxane (PDMS) precursors, hyaluronan (HA), pepsin (Pep), and glucose (Glu) were bought from Aladdin Reagent Company (Shanghai, China). Exonuclease I (Exo I) and bovine serum albumin (BSA) were purchased from Sangon Biotech Co., Ltd (Shanghai, China).

Instruments

XPS data were recorded with an X-ray photoelectron spectrometer (Thermo Electron, USA). The fluorescence lifetime and absolute fluorescence quantum yield were determined with an FLS920 fluorescence spectrophotometer (Edinburgh Instruments, England). Dynamic light scattering (DLS) and zeta potential measurements were conducted on a Zetasizer Nano ZS instrument (Malvern, England). Transmission electron microscopic (TEM) determinations were carried out on a JEM-2100F field emission electron microscope (JEOL, Japan). High-resolution TEM images, energy dispersive X-ray (EDX) elemental mapping, scanning transmission electron microscope (STEM) bright field image and selected area electron di□raction pattern (SAED) pattern were performed on a Tecnai G2 F20 S-TWIN microscopy (FEI,

Holland). Scanning electron microscopic (SEM) images and EDX analyses were acquired on an SU8020 ESEM microscope (Hitachi, Japan). Powder X-ray diffraction (PXRD) patterns were recorded in the range of 2θ = 5–80° using a D/Max-IIIC instrument (Rigaku, Japan) with Cu Kα radiation. Fourier-transform infrared (FT-IR) spectra were obtained by using a Thermo Nicolet 670 FT-IR instrument (Thermo Nicolet Corporation, USA) with the recorded range of 4000–450 cm^{-1}. TGA determinations were carried out with a Q500 thermal gravimetric analyzer (TA, USA). Ultraviolet photoelectron spectroscopic (UPS) spectra were carried out on a high resolution ultraviolet photoelectron spectrometer (PREVAC sp.z.0.0, Poland). All fluorescence measurements were performed on an RF5301 fluorescence spectrophotometer (Shimadzu Company, Japan). The measurements for the performance of the LED device were achieved on a high accurate array spectrometer (HSP6000, China). Ultrapure water was prepared by Millipore system (Milford, MA) and used throughout the experiments.

Preparation of GSH-CuNCs, Zn-HDS, and GSH-CuNCs/Zn-HDS

In a typical synthesis step, 0.046 g GSH was dissolved in 2.3 mL ultrapure water and then frozen in a freezer for 10 min to form ice-water mixture. Subsequently, 200 μL NaOH solution (1 M) was dropped into GSH solution accompanied with vigorous shaking. 2.5 mL $Cu(NO_3)_2$ solution (10 mM) was added into GSH solution and then the mixture was vigorously stirred for 5 min. The final solution went from black green to light yellow, indicating the formation of GSH-CuNCs. The products were centrifuged at 12000 rpm for 10 min to remove the aggregates.

In order to synthesize Zn-HDS, 8.925 g $Zn(NO_3)_2 \cdot 6H_2O$ was dissolved in 20 mL ultrapure water, subsequently 1 g ZnO powder was added into the solution. The

mixture was stirred at room temperature for 5 days. The obtained solids were filtered and washed for three times and then dried at 60 °C for 24 h in a vacuum drying oven. The obtained white solid is the product Zn-HDS.

0.02 g Zn-HDS was added into 20 mL ultrapure water and then subjected to ultrasonic treatment for 1 h to disperse uniformly. 200 μL GSH-CuNCs (18 $mg \cdot mL^{-1}$) and 2.16 mL Zn-HDS suspension (1 $mg \cdot mL^{-1}$) were add into 2.64 mL ultrapure water, and the mixture was allowed to react at room temperature for 48 h. Afterwards, the fluorescence of the mixture changed from dark to bright orange, suggesting the formation of GSH-CuNCs/Zn-HDS fluorescence composite. After centrifuged and washed for three times, GSH-CuNCs/Zn-HDS was dried in a vacuum drying oven at 60 °C to form solid powder.

Preparation of LDH and GSH-CuNCs/LDH

The process of hydrothermal synthesis of LDH was referred to an as-reported method.[1] Typically, 0.721 g urea, 0.375 g $Al(NO_3)_3 \cdot 9H_2O$, and 0.513 g $Mg(NO_3)_2 \cdot 6H_2O$ were dissolved in 70 mL ultrapure water. The solution was heated at 100 °C for 24 h in a 100 mL teflon-lined stainless steel autoclave. The solid product was washed with ultrapure water for thrice and dried in air at 60 °C. 0.3 g product, 42.495 g $NaNO_3$, and 66.67 μL HNO_3 were treated with 300 mL ultrapure water and shaken for 1 day at ambient temperature (25 °C) whilst purging with nitrogen gas. The resulting product was washed with hot ultrapure water and then dried in a vacuum at 60 °C.

0.02 g LDH was add into 20 mL ultrapure water and then subjected to the ultrasonic treatment for 30 min to disperse uniformly. 200 μL GSH-CuNCs (18 $mg \cdot mL^{-1}$) and 2.16 mL LDH suspension (1 $mg \cdot mL^{-1}$) were add into 2.64 mL

ultrapure water, and the mixture was vigorously shaken for 10 min. After that, the fluorescence of the mixture changed from dark black to bright orange, suggesting the formation of GSH-CuNCs/LDH.

Detection of GLU based on GSH-CuNCs/Zn-HDS

50 μL PNPG (10 mM) and 50 μL GLU with different activities were introduced into 1.9 mL ultrapure water. After incubation for 90 min at 37 °C, 20 μL NaOH (1 M) was introduced to make the final solution. It was observed that the solution changed from colorless to yellow. Subsequently, 50 μL above solutions, 50 μL PBS (0.1 M, pH 6.0), and 400 μL ultrapure water were added into 2.5 mL GSH-CuNCs/Zn-HDS (2 $mg \cdot mL^{-1}$) under vigorous shaking for 2 min. Finally, the fluorescence spectra of the mixture were recorded with a fluorescence spectrophotometer. Each concentration of GLU (0, 0.25, 0.5, 0.75, 1, 1.5, 2, 3, 4, 5, 6, 7, 8, 9 $U \cdot L^{-1}$) was detected with new sample, and each experiment was repeated three times. To evaluate the selectivity of the fluorescence assay for HAase, some potential interferences such as Na^+, K^+, Mg^+, Ca^{2+}, PO_4^{3-}, GSH, Cys, urea, Glu, BSA, CS, HA, Thr, AChE, Exo I, GR, Lys, Pep, and Try were individually investigated under the same conditions.

Application to real samples

Five liver cancer human serum samples and five healthy human serum samples were collected from the First Hospital of Jilin University (Changchun, China) with informed consent from human subjects. All experiments were performed in accordance with the Guidelines of Jilin University and approved by the Ethics Committee of Jilin University. Firstly, to remove the impurities, the serum samples were centrifuged at 10000 rpm for 20 min. Then, GLU with different concentrations

were added into the serum samples to prepare the spiked samples. Subsequently, 1.0 mL serum samples containing various amounts of GLU, 10 mM PNPG and 10 μL NaOH (1 M) were incubated for 90 min at 37 °C. 300 μL above serum sample, 50 μL PBS (0.1 M, pH 6.0), and 150 μL ultrapure water were added into 2.5 mL GSH-CuNCs/Zn-HDS (2 $mg \cdot mL^{-1}$), and the mixture was vigorously shaken for 2 min. The fluorescence of the resulting samples was measured with a fluorescence spectrophotometer.

Fabrication of LED based on GSH-CuNCs/Zn-HDS powder

GaN LED chips with 365 nm UV emission were bought from Advanced Optoelectronic Technology Co., Ltd (Zhenjiang, China), and the chips were operated at a voltage of 4.0 V to provide excitation light. GSH-CuNCs/Zn-HDS fine powder was mixed with PDMS precursors with the ratio of 5:15 (*w*/*w*). To remove bubbles, the mixture was put into a vacuum chamber before loaded on the LED chip. Subsequently, the mixture was cured at 60 °C for 2 h to construct the LED chip.

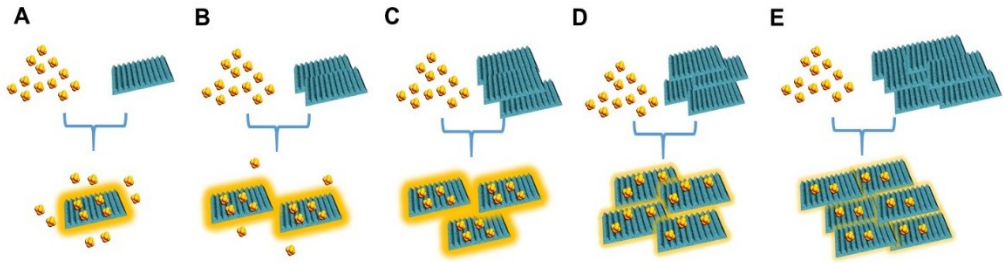

Scheme S1 Mechanism of fluorescence intensity of GSH-CuNCs/Zn-HDS over the ratio of Zn-HDS to GSH-CuNCs.

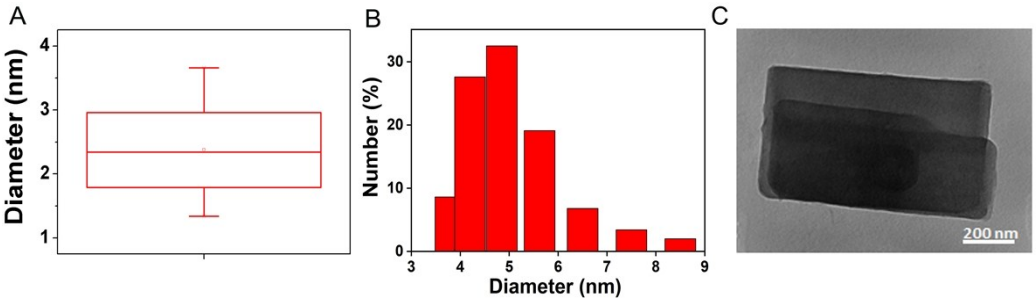

Fig. S1 (A) BOX plot of size distribution of GSH-CuNCs. (B) Size distribution of GSH-CuNCs by DLS. (C) TEM image of single Zn-HDS.

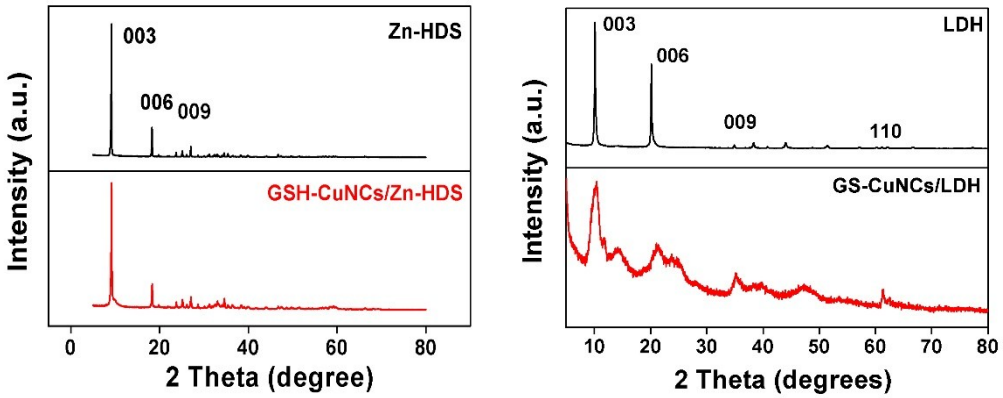

Fig. S2 (A) XRD patterns of Zn-HDS and GSH-CuNCs/Zn-HDS. (B)XRD patterns of LDH and GSH-CuNCs/LDH.

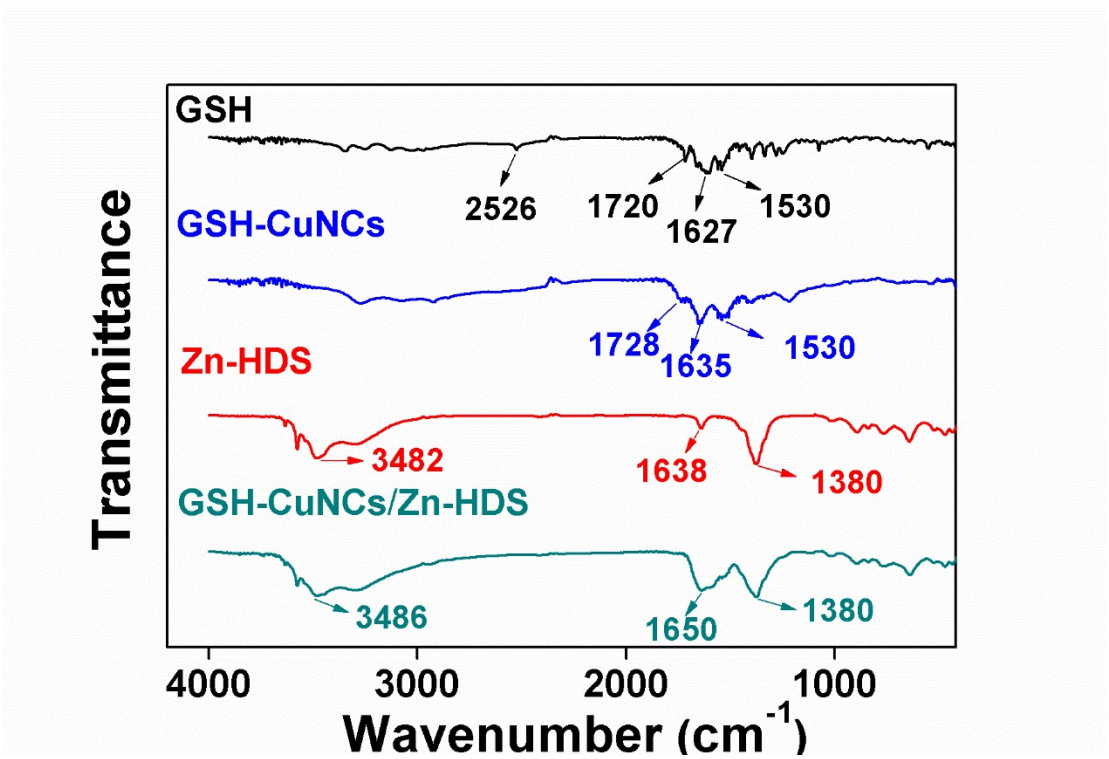

Fig. S3 FTIR spectra of GSH, GSH-CuNCs, Zn-HDS and GSH-CuNCs/Zn-HDS.

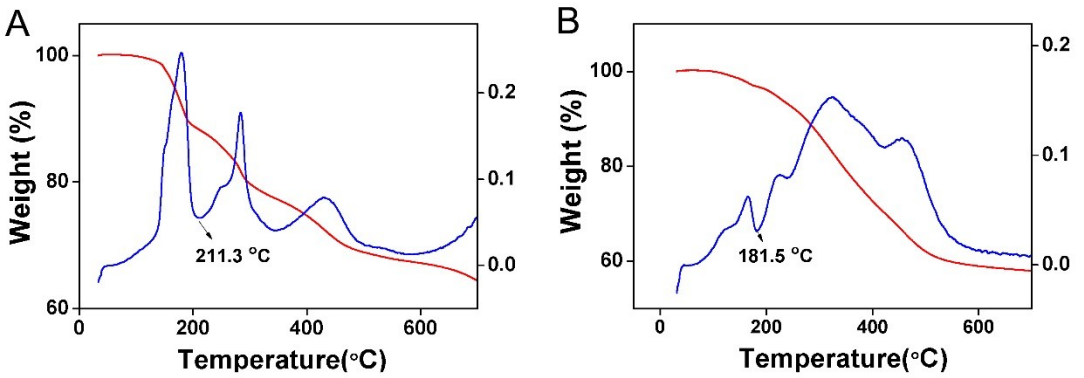

Fig. S4 TGA curves of (A) GSH-CuNCs/Zn-HDS and (B) GSH-CuNCs/LDH.

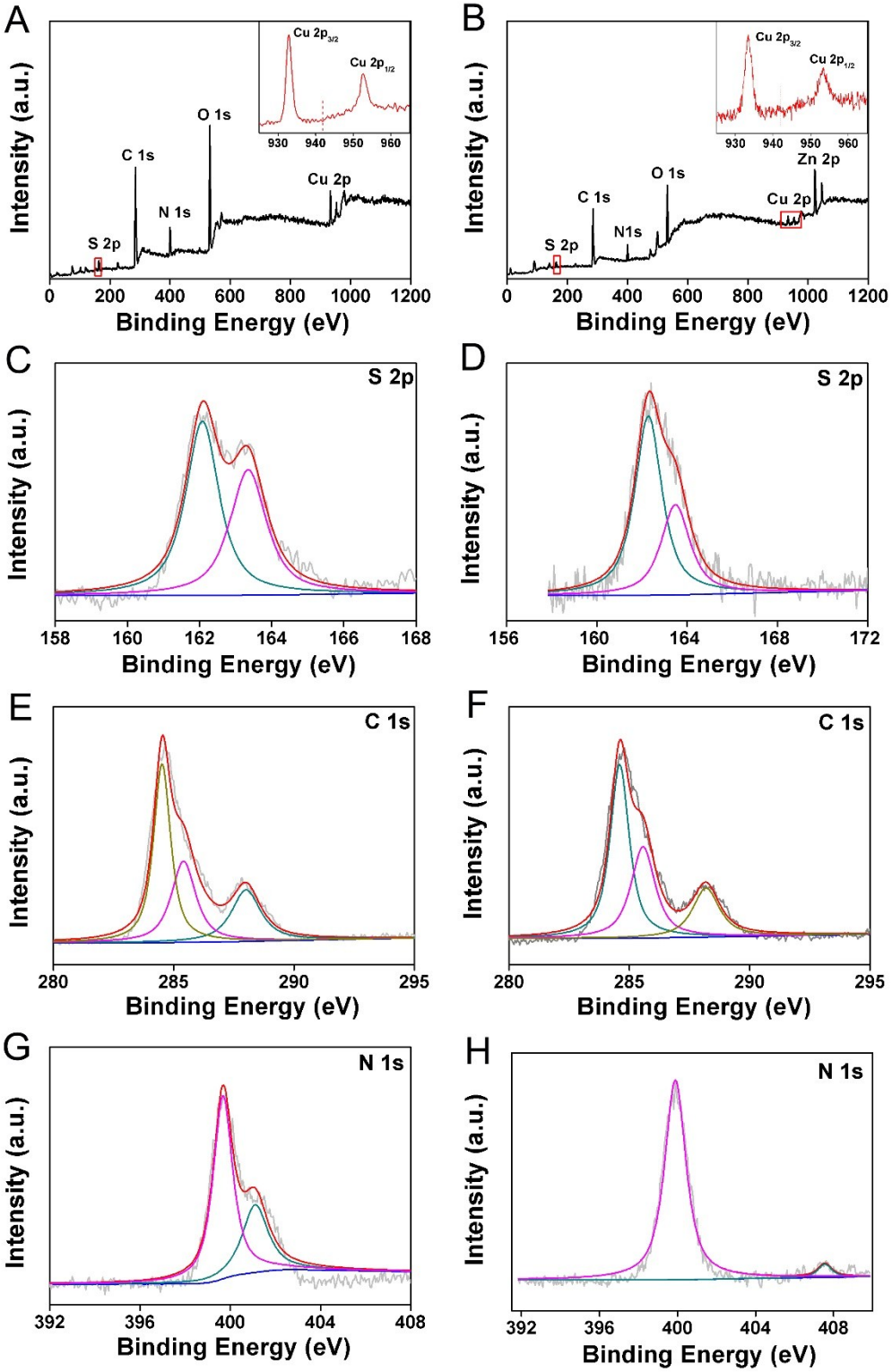

Fig. S5 XPS spectra of (A) GSH-CuNCs and (B) GSH-CuNCs/Zn-HDS. S 2p XPS spectra of (C) GSH-CuNCs and (D) GSH-CuNCs/Zn-HDS. C 1s XPS spectra of (E) GSH-CuNCs and (F) GSH-CuNCs/Zn-HDS. N 1s XPS spectra of (G) GSH-CuNCs and (H) GSH-CuNCs/Zn-HDS.

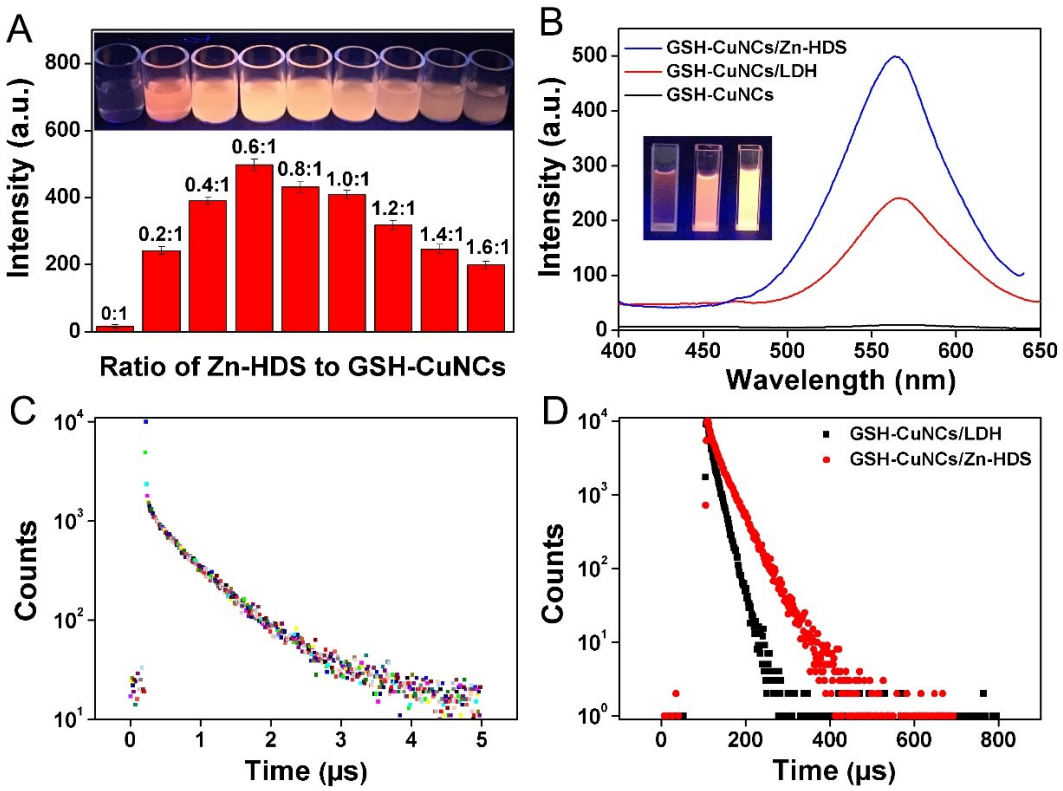

Fig. S6 (A) Fluorescence intensity of GSH-CuNCs/Zn-HDS at different ratios (by weight) of Zn-HDS to GSH-CuNCs. Inset: The digital photo of GSH-CuNCs/Zn-HDS at different ratios of Zn-HDS to GSH-CuNCs. (B) Fluorescence spectra GSH-CuNCs, GSH-CuNCs/LDH and GSH-CuNCs/Zn-HDS. Inset: The digital photo of GSH-CuNCs, GSH-CuNCs/LDH, and GSH-CuNCs/Zn-HDS. Typical fluorescence decay curves of (C) GSH-CuNCs and (D) GSH-CuNCs/LDH and GSH-CuNCs/Zn-HDS.

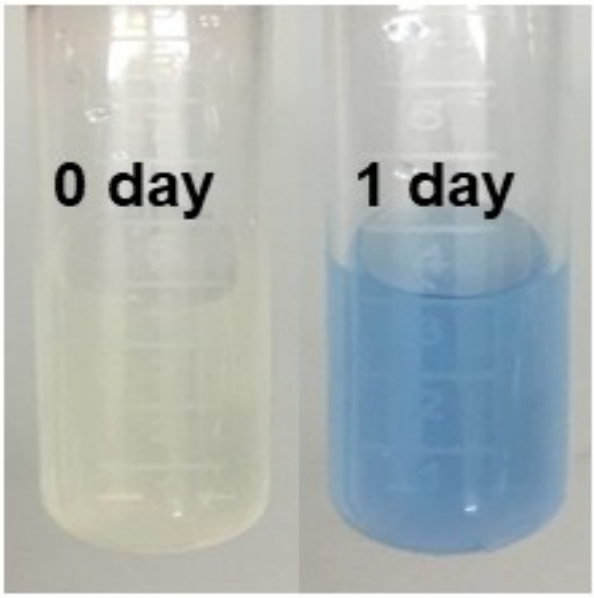

Fig. S7 Digital photo of GSH-CuNCs stored for 0 day and 1 day at room temperature.

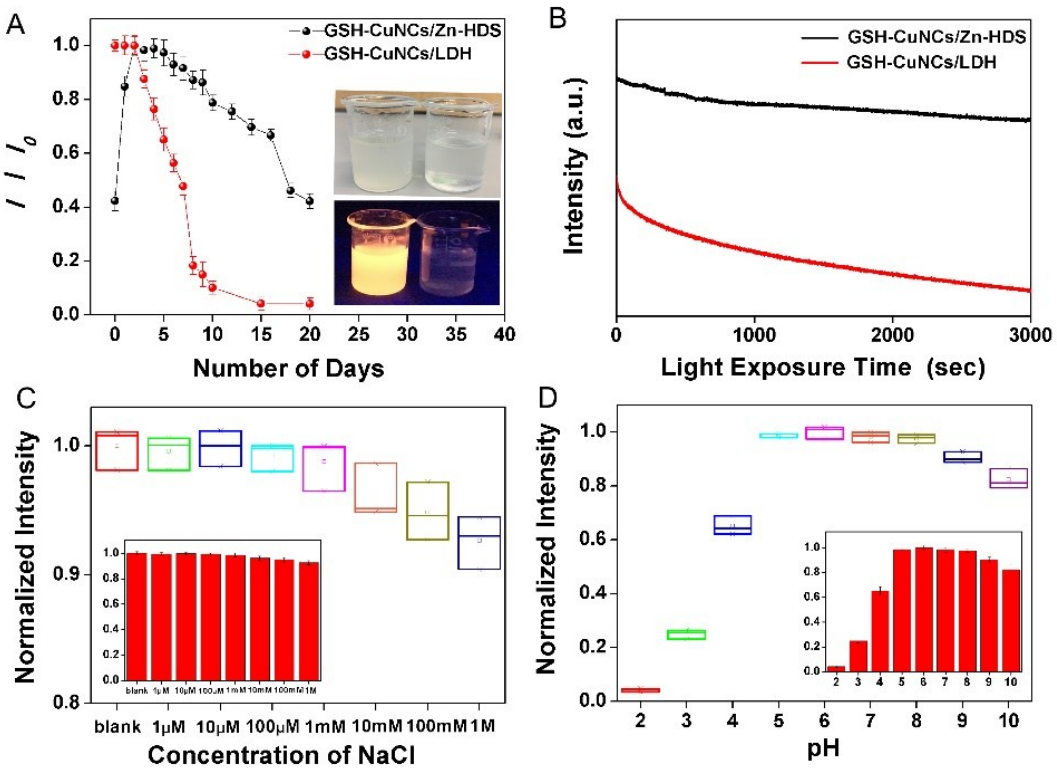

Fig. S8 (A) 20-day fluorescence intensity of GSH-CuNCs/Zn-HDS (black) and GSH-CuNCs/LDH (red). (I_0 is the initial fluorescence and I is the fluorescence intensity during different days). Inset: Digital photos of GSH-CuNCs/Zn-HDS (left) and GSH-CuNCs/LDH (right) stored for 20 days under natural light and UV light. (B) Fluorescence intensity of GSH-CuNCs/Zn-HDS (black) and GSH-CuNCs/LDH (red) exposed for 3000 second under excitation. (C) Fluorescence intensity of GSH-CuNCs/Zn-HDS after adding NaCl with various concentrations. (D) Fluorescence intensity of GSH-CuNCs/Zn-HDS at different pH values.

Fig. S9 Digital photo of solid GSH-CuNCs/Zn-HDS (left) and GSH-CuNCs/LDH (right) stored for two month under UV light.

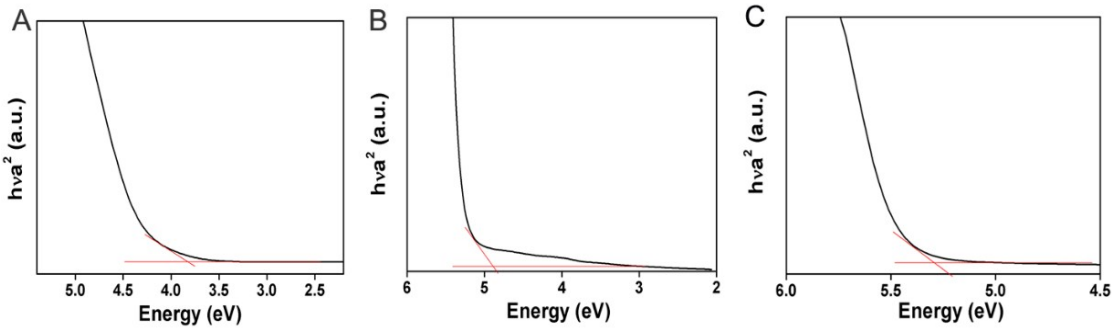

Fig. S10 Band gap energies of (A) GSH-CuNCs, (B) LDH, and (C) Zn-HDS.

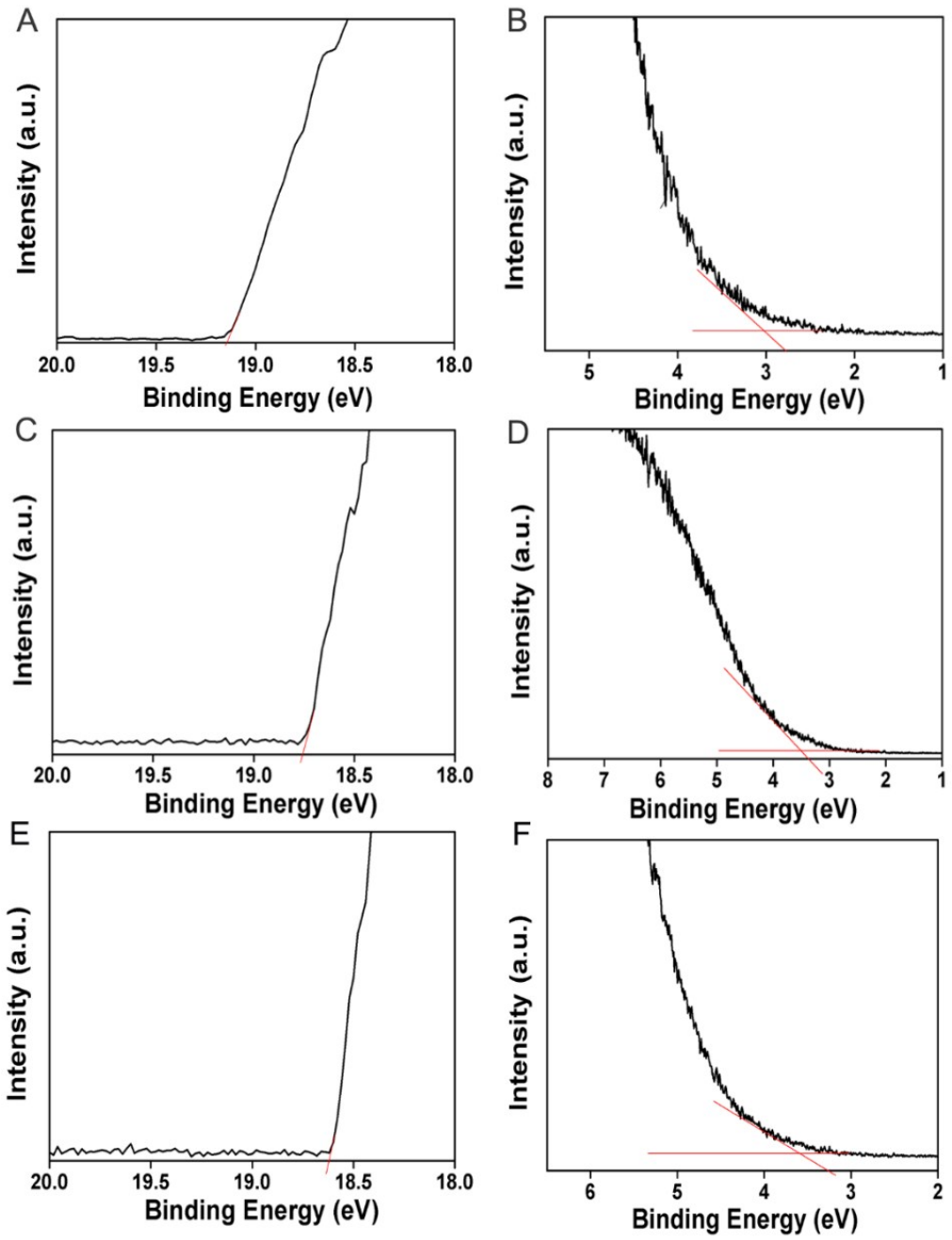

Fig. S11 UPS spectra of (A), (B) GSH-CuNCs; (C), (D) LDH; (E), (F) Zn-HDS.

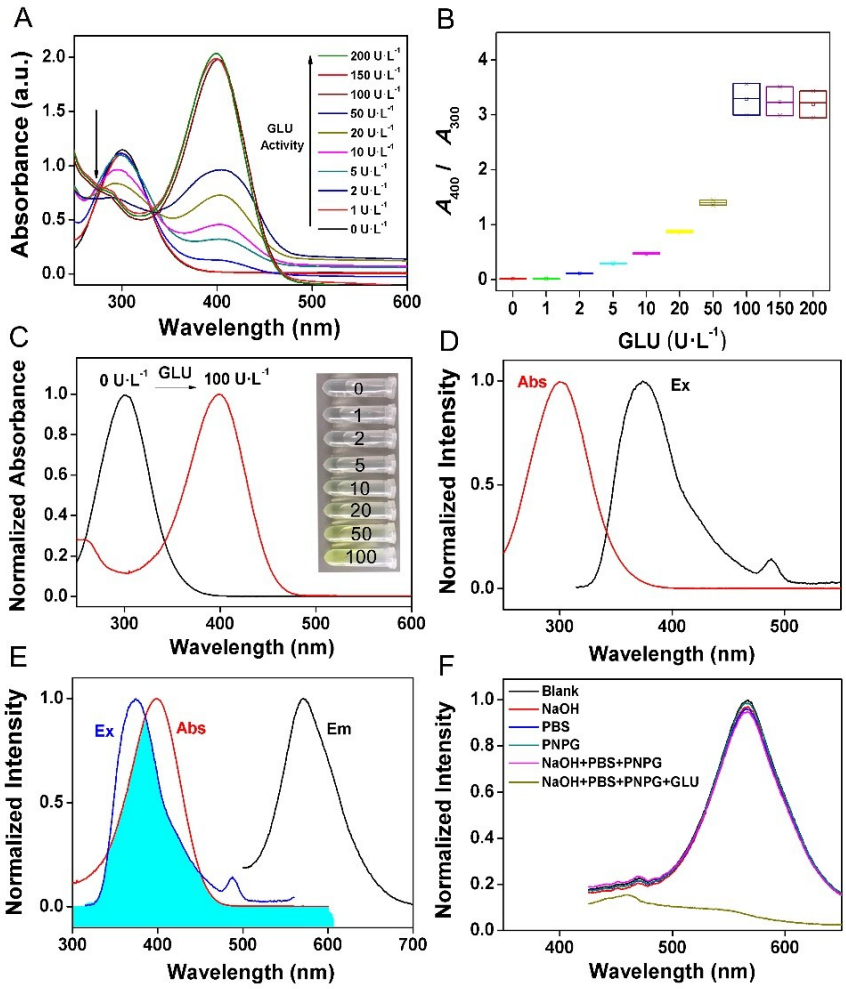

Fig. S12 (A) UV-vis absorption spectra of enzymatic reaction solutions containing GLU with different activities. (B) BOX plot of UV-vis absorption ratio versus GLU concentrations (A_{400} and A_{300} are the absorbance of enzymatic reaction solutions at 400 and 300 nm). (C) Normalized absorption spectra when GLU concentrations are 0 and 100 $U \cdot L^{-1}$ (inset: digital photos of enzyme reaction solutions). (D) UV-vis absorption spectrum of PNPG (red) and fluorescence excitation spectrum of GSH-CuNCs/Zn-HDS (black). (E) UV-vis absorption spectrum of PNP (red), fluorescence excitation (blue) and emission (black) spectra of GSH-CuNCs/Zn-HDS. (F) Fluorescence emission spectra of GSH-CuNCs/Zn-HDS in the presence of other substances.

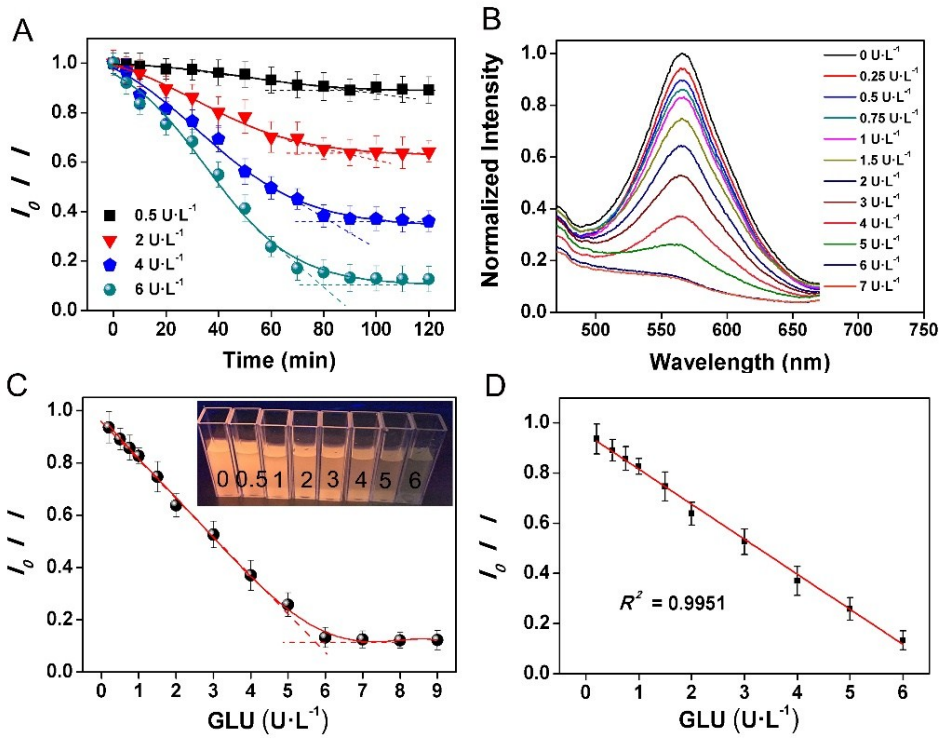

Fig. S13 (A) Relative fluorescence ratios of GSH-CuNCs/Zn-HDS versus the hydrolysis time of GLU with di□erent concentrations. (B) Fluorescence emission spectra of GSH-CuNCs/Zn-HDS sensing system in the presence of GLU with different activities. (C), (D) Linear relationship between fluorescence intensity and GLU activities. (I and I_0 are fluorescence intensities of GSH-CuNCs/Zn-HDS in the presence and absence of GLU).

The images of samples were captured by a smartphone camera (iPhone 6s, Apple Inc., USA). The colors of the images were converted into data then read out by the image processing application (Color Analyzer), then analyzed by a data analysis application (Regression). Lab color mode (L represents Luminosity; a represents a range from magenta to green; and b represents a range from yellow to blue) was introduced. The fluorescence intensity decreased as GLU activities increased, therefore, a calibration curve with $R^2 = 0.9899$ was obtained between L values and the activities of GLU. The linear range was from 0.5 to 6 $U \cdot L^{-1}$ with a detection limit of 0.30 $U \cdot L^{-1}$.

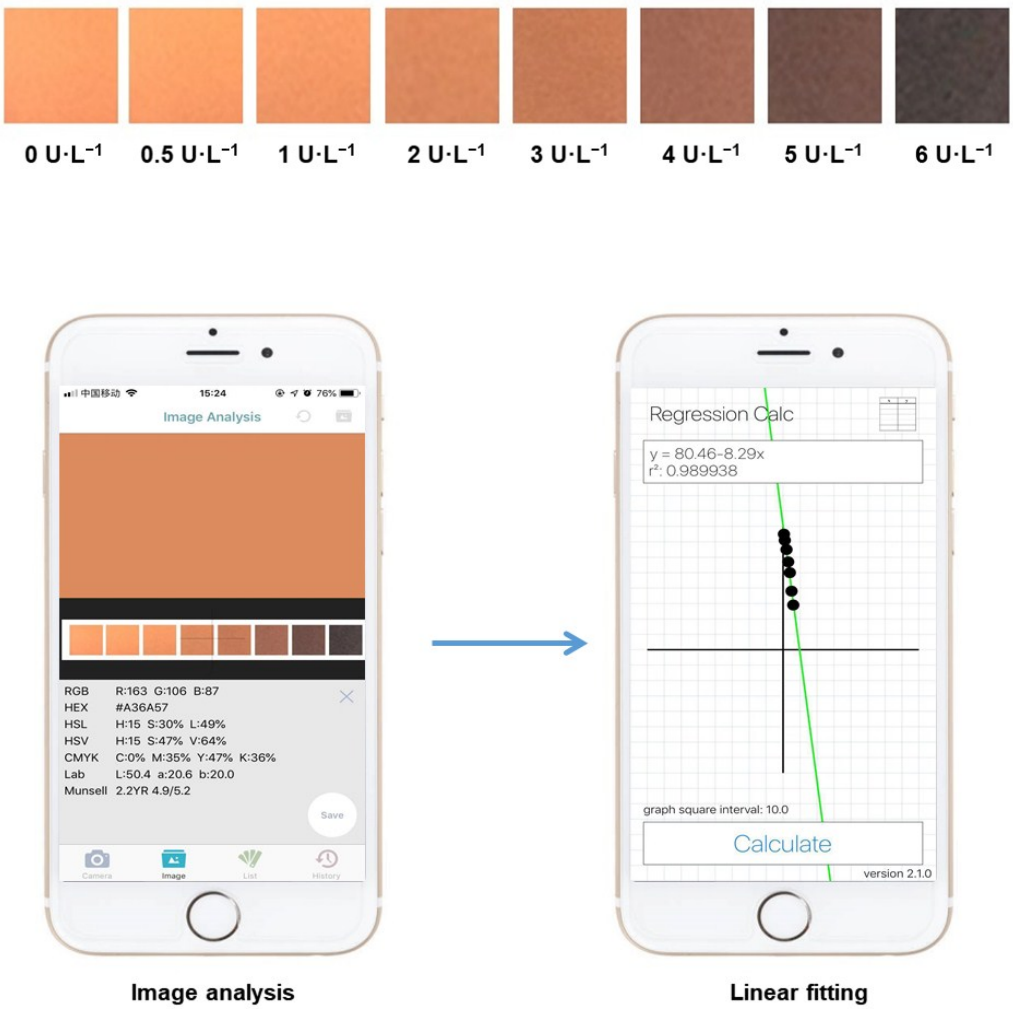

Fig. S14 Illustration of quantitative detection of GLU by smartphone.

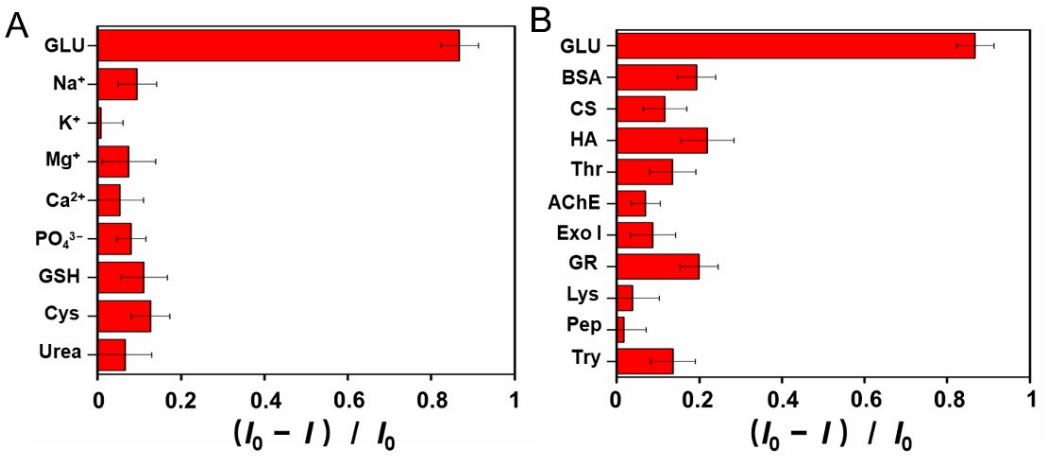

Fig. S15 Selectivity of GSH-CuNCs/Zn-HDS sensing system for GLU.

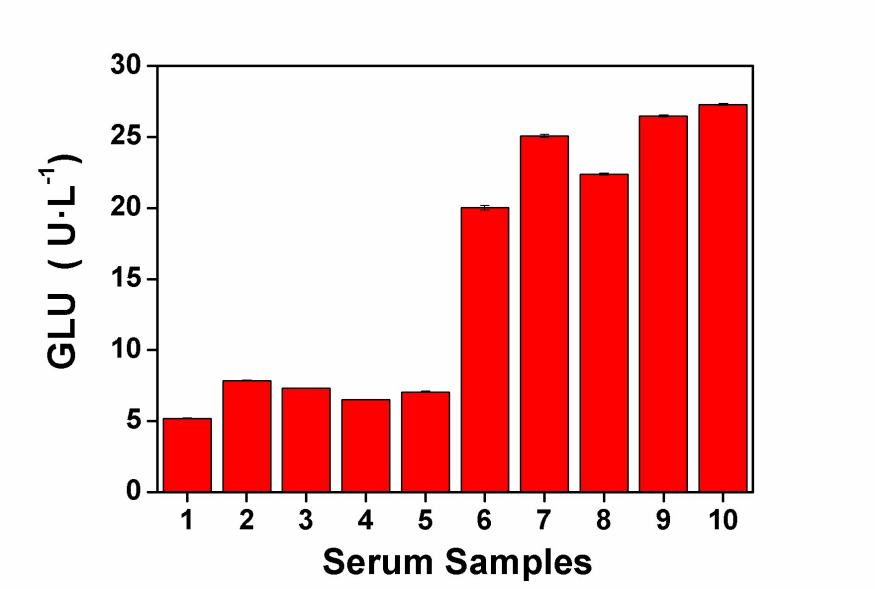

Fig. S16 Analytical results of the GSH-CuNCs/Zn-HDS-based fluorescence method for the detection of GLU (1–5 represented healthy serum samples, 6–10 represented liver cancer serum samples).

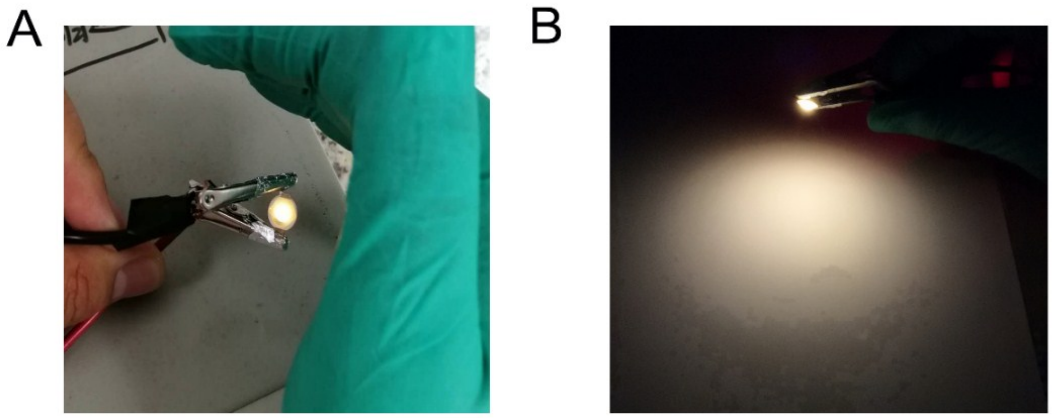

Fig. S17 Digital photos of LED.

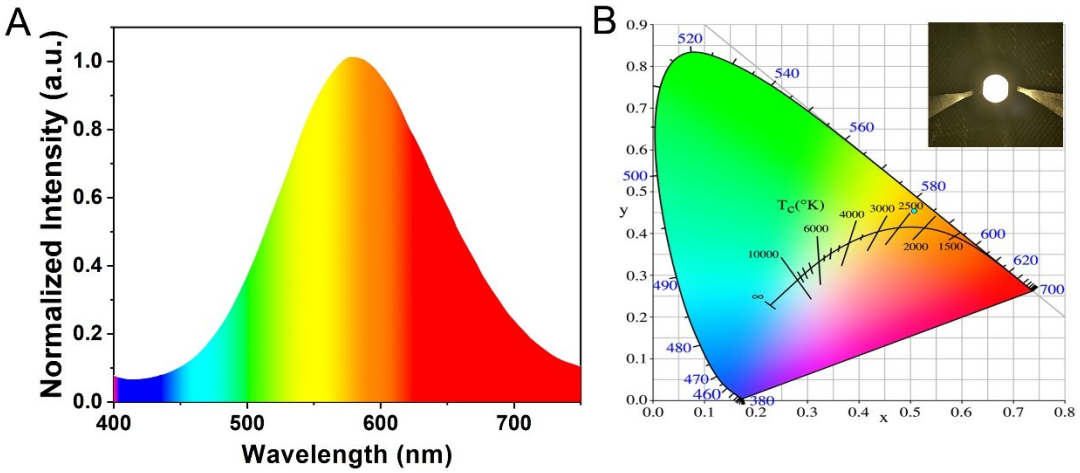

Fig. S18 (A) Emission spectrum and (B) CIE diagram of LED under a voltage of 3.3 V and driven current of 50 mA. Inset: Digital photo of LED.

Table S1. Cu, S, and C content in GSH-CuNCs/Zn-HDS at different ratios of Zn-HDS to GSH-CuNCs.

Ratio (w/w)	Cu Content (%)	S Content (%)	C Content (%)	Fluorescence Intensity (a.u.)
0.2:1	0.82	0.42	11.76	241.45
0.4:1	0.87	0.46	11.86	390.51
0.6:1	2.09	1.11	14.52	498.21
1.0:1	1.24	0.59	11.87	409.42
1.6:1	0.73	0.38	9.70	199.36

Three-exponential function was used to fit the fluorescence decay curves of GSH-CuNCs and the double-exponential function was suitable for GSH-CuNCs/LDH. Decay in the fluorescence intensity of (I) with time (t) was fitted by the following functions.

Three-exponential fit:

$$I = A_1 e^{-t/\tau_1} + A_2 e^{-t/\tau_2} + A_3 e^{-t/\tau_3} \quad (1)$$

Double-exponential fit:

$$I = A_1 e^{-t/\tau_1} + A_2 e^{-t/\tau_2} \quad (2)$$

The weighted mean lifetime (<τ>) was calculated according to the following equation:

$$<\tau> = \frac{A_1\tau_1 + A_2\tau_2 + A_3\tau_3}{A_1 + A_2 + A_3} \quad (3)$$

where τ_i (i =1, 2, 3) was the lifetimes of shorter- or longer-lived species, A_i (i =1, 2, 3) were their respective amplitudes and χ^2 indicate the goodness of the fit.

Table S2. The fitting of fluorescence decay data of GSH-CuNCs, GSH-CuNCs/LDH, and GSH-CuNCs/Zn-HDS.

Samples	τ_i (μs)	A_i (%)	<τ> 4 (μs)	χ^2
GSH-CuNCs	0.0041	32.03	0.42	1.044
	0.1243	7.66		
	0.6744	60.31		
GSH-CuNCs/LDH	4.892	15.39	16.30	0.979
	18.37	84.61		
GSH-CuNCs/Zn-HDS	6.32	17.33	16.56	1.249
	18.71	82.67		

Table S3. Comparison of different detection methods for GLU.

Detection Method	Linear range ($U\ L^{-1}$)	LOD ($U\ L^{-1}$)	Ref.
Amperometric assay / Carbon sensors	5-2500	5	2
Colorimetry	–	–	3
Fluorescence / Carbon dots	1-60	0.30	4
Fluorescence / RhB@MOF-5	0.1-10	0.03	5
Phosphorescent assay / Quantum dots	10-300	7	6
Fluorescence / CuNCs/Zn-HDS	0.5–6	0.22	This work
Smartphone / CuNCs/Zn-HDS	0.5–6	0.30	This work

Table S4. Results of the determination of GLU in seven healthy human serum samples.

Sample	Found ($U \cdot L^{-1}$)	Added ($U \cdot L^{-1}$)	Detected ($U \cdot L^{-1}$)	Recovery (%)	RSD ($n = 3$, %)
Serum 1	5.18	5.0	10.51	106.6	3.5
		10.0	14.89	97.1	2.6
Serum 2	7.83	5.0	13.18	107.0	3.2
		10.0	18.43	106.0	1.7
Serum 3	7.29	5.0	12.07	95.6	4.3
		10.0	18.45	111.6	3.7
Serum 4	6.50	5.0	11.56	101.2	3.6
		10.0	17.03	105.3	2.8
Serum 5	7.04	5.0	12.25	104.2	2.9
		10.0	16.88	98.4	3.5

Table S5. Photoelectric parameters of LED operating at different current.

Current (mA)	CIE	CCT (K)	Ra	LE (lm/W)	CP (%)
20	(0.51, 0.45)	2327	73.1	1.50	88.2
50	(0.51 0.45)	2461	73.5	1.56	85.0
100	(0.49, 0.46)	2656	74.2	1.47	85.7
200	(0.46, 0.47)	3115	74.0	1.42	85.2

References

1 D. Yan, J. Lu, M. Wei, J. Han, J. F. Ma and D. G. Evans, *Angew. Chem.,* 2009, **48**, 3073-3076.

2 M. Rochelet, S. Solanas, L. Betelli, B. Chantemesse, F. Vienney and A. Hartmann, *Anal. Chim. Acta* 2015, **892**, 160-166.

3 N. Waszkiewicz, S.D. Szajda, E. Konarzewska-Duchnowska, B. Zalewska-Szajda, R. Gałązkowski and A. Sawko, *Postepy. Hig. Med. Dosw.* 2015, **69**, 436-439.

4 S. Lu, G. Li, Z. Lv, N. Qiu, W. Kong, and P. Gong, *Biosens. Bioelectron.* 2016, **85**, 358-362.

5 L. Guo, Y. Liu, R. Kong, G. Chen, H. Wang and X. Wang, *Sens. Actuators B-Chem.* 2019, **295**, 1-6.

6 D.D. Tang, J.Y. Zhang, X.D. Hou and P. Wu *Chinese. J. Anal. Chem.* 2017, **45,** 1909-1914.